Monatsh Chem (2009) 140:1431–1436
DOI 10.1007/s00706-009-0199-2

ORIGINAL PAPER

Structural variations of nickel complexes in NiS_4 and NiS_2PN coordination environments: spectral and single-crystal X-ray structural studies on bis(4-methylpiperidinecarbodithioato-*S*,*S*′)nickel(II) and (4-methylpiperidinecarbodithioato-*S*,*S*′)(thiocyanato-*N*)(triphenylphosphine)nickel(II)

N. Srinivasan · V. Sathyaselvabala · K. Kuppulekshmy · P. Valarmathi · S. Thirumaran

Received: 30 April 2009 / Accepted: 11 October 2009 / Published online: 18 November 2009

Abstract [Ni(4-mpipdtc)$_2$] and [Ni(4-mpipdtc)(PPh_3)(NCS)] (4-mpipdtc = 4-methylpiperidinecarbodithioate anion) have been characterized by electronic, IR, and NMR spectroscopy, single crystal X-ray analysis, and cyclic voltammetry. IR spectra of the complexes show the contribution of the thioureide form to the structures. ^{1}H NMR spectra show the deshielding of α-CH_2 protons on complexation. ^{13}C NMR spectra shows interesting differences between the N$^{13}CS_2$ carbon signals of the parent complex [Ni(4-mpipdtc)$_2$] and the mixed ligand complex [Ni(4-mpipdtc)(PPh_3)(NCS)]. The N$^{13}CS_2$ carbon signal for [Ni(4-mpipdtc)(PPh_3)(NCS)] is observed at 204.85 ppm with an upfield shift of about 3.8 ppm compared with that found in [Ni(4-mpipdtc)$_2$] (201.06 ppm). The observed shielding in [Ni(4-mpipdtc)(PPh_3)(NCS)] indicates the effect of PPh_3 on the mesomeric drift of electron density toward nickel through the thioureide C–N bond. Single crystal X-ray analysis of [Ni(4-mpipdtc)$_2$] and [Ni(4-mpipdtc)(PPh_3)(NCS)] confirms the presence of four-coordinated nickel in a distorted square-planar arrangement with the NiS_4 and NiS_2PN chromophores, respectively. The C–N (thioureide) bond lengths of [Ni(4-mpipdtc)(PPh_3)(NCS)] are shorter than those found in [Ni(4-mpipdtc)$_2$], because of the presence of the π-acid (triphenylphosphine) in [Ni(4-mpipdtc)(PPh_3)(NCS)]. Significant asymmetry in Ni–S bond distances was observed in Ni(4-mpipdtc)(PPh_3)(NCS)] (2.162(2) and 2.211(2) Å). This observation clearly supports the less effective trans effect of SCN^- over PPh_3. The piperidine ring in the dithiocarbamate fragment is in the normal chair conformation.

Keywords Heterocyclic dithiocarbamates · Triphenylphosphine · Thiocyanate · Nickel

N. Srinivasan · V. Sathyaselvabala · K. Kuppulekshmy · P. Valarmathi · S. Thirumaran (✉)
Department of Chemistry, Annamalai University, Annamalinagar 608 002, Tamil Nadu, India
e-mail: sthirumaran@yahoo.com

Introduction

Dithiocarbamato complexes of the transition metal ions continue to attract the attention of researchers [1, 2]. Diverse applications as catalysts [3–5] and in the medicinal field [6] is inherent to nickel(II) complexes with simple and chelating phosphines. Divalent nickel complexes of dithiocarbamates with different substituents contain planar diamagnetic MS_4 chromophores [7, 8]. Ni(II) dithiocarbamates show interesting variations in their reactions with Lewis bases such as phosphines and hard bases such as nitrogenous ligands [9, 10]. The symbiotically induced softness and the electronic effects of the substituents on the dithiocarbamate ligands were found to be important in deciding the reactivity [11, 12]. The effect of free and chelating phosphines on the NiS_2P_2 chromophore and on the thioureide C–N bond have been studied earlier [13]. The objective of this work was a detailed study of the coordination compounds [Ni(4-mpipdtc)$_2$] and [Ni(4-mpipdtc)(PPh_3)(NCS)], to determine the effect of the P-donor atom on the structure and properties of the complex.

Results and discussion

IR and electronic spectral studies

The IR spectrum of **2** shows the thioureide $\bar{\nu}_{C-N}$ band at 1,544 cm^{-1}. The shift in $\bar{\nu}_{C-N}$ (thioureide) values to

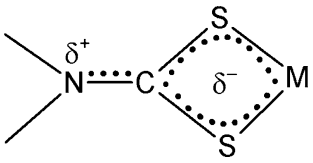

Scheme 1

a higher wavenumber compared with parent complex **1**, observed at 1,510 cm^{-1}, is because of the mesomeric drift of electron density from the dithiocarbamate ligand towards the metal atom and this increases the contribution of the polar thioureide form in **2**. The $\bar{\nu}_{C-S}$ (dithiocarbamate) appears at 964 cm^{-1} for **1** and 965 cm^{-1} for **2** without any splitting, supporting the bidentate coordination of the dithiocarbamate moiety [14]. The bands observed for complex **2** at 2,098 and 848 cm^{-1} are connected with $\bar{\nu}_{C\equiv N}$ and $\bar{\nu}_{C-S}$ vibrations, which confirm the coordination of the NCS group through the nitrogen atom [15].

The electronic spectrum of **2** shows a band at 483 nm which can be attributed to the d–d electron transitions for Ni(II) square planar complexes [16]. The bands observed at 326, 270, and 250 nm arise from intraligand π–π^* charge-transfer transitions mainly associated with N–C=S and S–C=S groups [17].

NMR spectral studies

For both complexes, ^{1}H NMR signals around 2.90 and 4.50 ppm arise from the axial and equatorial protons at C-2, respectively. The observed deshielding of the protons adjacent to nitrogen in both complexes [18] is attributed to release of electrons by the NR_2 groups, forcing electron density toward sulfur (or the metal) via the thioureide system. For the mixed ligand complex **2**, the aromatic protons resonate in the region 7.43–7.68 ppm.

The most important ^{13}C NMR chemical shift value of the thioureide carbon atom $S_2^{13}CN$ is observed at 204.85 and 201.06 ppm for complexes **1** and **2**, respectively. The $S_2^{13}CN$ carbon signal observed for **2** is additionally shielded by 3.8 ppm compared with the parent complex **1**. Because there is a contribution of the double bond character to a formally single N–C bond in the dithiocarbamate group, i.e. the admixture of sp^2-hybridized state to sp^3 orbitals of the nitrogen atom, a substantial δ^+ surplus charge is localized on the nitrogen atom whereas a δ^- charge is delocalized through the four-membered metalochelate ring-CS_2M [19] (Scheme 1). The presence of a π-acid (triphenylphosphine) in **2** increases the mesomeric drift of electron density from the dithiocarbamate moiety toward the metal atom. This yields an increase in the $N^{\delta+}\cdots C^{\delta-}$ partial double bond character and, as a result, displacement of the electron density from the nitrogen to the carbon atom of the dithiocarbamate group [20]. This explains the additional shielding of carbon sites in the –N–C(S)S group of **2**. This observation is supported by the higher $\bar{\nu}_{C-N}$ value observed in the IR spectrum of the complex **2**.

Structural analysis

The ORTEP diagram of **1** is shown in Fig. 1. The complex is monomeric and discrete. Four units of [Ni(4-mpipdtc)$_2$] are present in the unit cell. Because of the small bite angles associated with the dithiocarbamate moiety (S1–Ni–S2 = 79.16(4)° and S3–Ni–S4 = 79.04°), the NiS_4 chromophore is not of perfectly square planar arrangement. The Ni–S distances lie in the expected range for four-coordinated dithiocarbamates [21]. The C–S distances (1.710(4) Å) are similar to those observed in other dithiocarbamate complexes, which confirms the substantial double-bond character associated with the C–S bonds. The short thioureide C–N distance (1.310(5) Å) indicates that the π-electron density is delocalized over the S_2CN moiety and that this bond has double-bond character comparing well with the adjacent typical single bonded N–C distance (C(3)–N(1) = 1.457(5) Å).

[Ni(4-mpipdtc)(PPh_3)(NCS)] is discrete and monomeric. Four formula units are present in the unit cell. The ORTEP diagram is shown in Fig. 2. Complex **2** exists in two isomeric forms. One of these, hereafter denoted as A, contains atom Ni(1) whereas B involves atom Ni(2). The molecules A and B have different bond properties. However, comparison of the bond properties associated with A is valid for B. Therefore, in the following discussion, properties associated with A are considered for comparison. The observed distortion of the square planar coordination around nickel is attributed to the small bite angle of 79.08(8)°. The

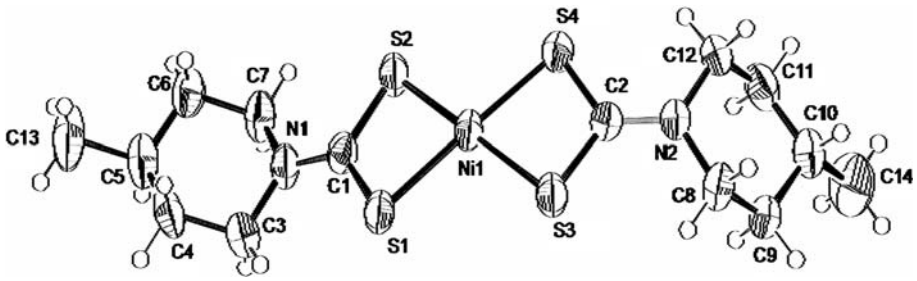

Fig. 1 ORTEP diagram of [Ni(4-mpipdtc)$_2$] (**1**)

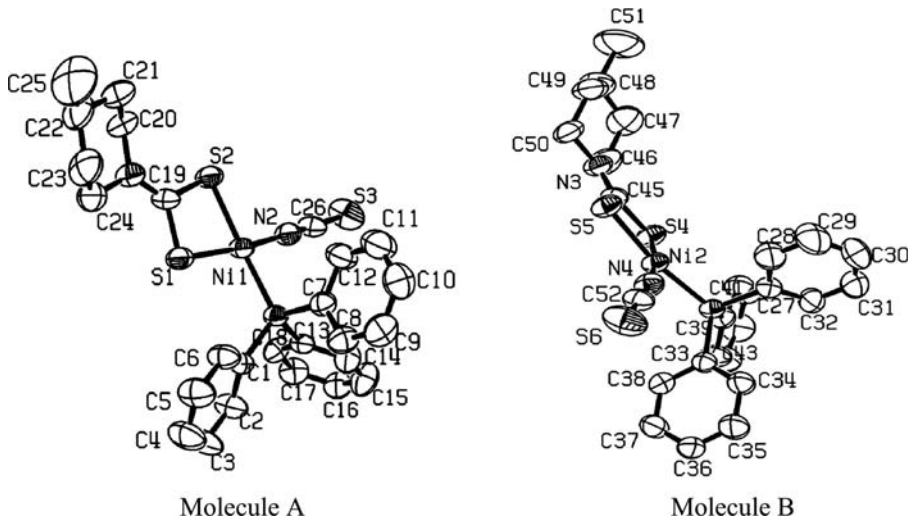

Fig. 2 ORTEP diagrams of [Ni(4-mpipdtc)(PPh_3) (NCS)] (**2**)

observed difference in Ni–S distances (2.162(2) and 2.211(2) Å) is because of the different trans-influencing properties of PPh_3 and NCS^-. PPh_3, being a good π acceptor, has a greater trans effect and hence the Ni–S bond trans to PPh_3 is longer than the other Ni–S bond.

The Ni–N distance (1.868(7) Å) is quite short, showing the effective bonding between the nickel atom and the thiocyanate-N. The C–N bond distance in the thiocyanate group (1.140(9) Å) is significantly shorter than the thioureide C–N bond distance of 1.282(10) Å. The C–S bond length in the thiocyanate group is 1.616(9) Å, which is similar to the C=S distance of 1.69 Å. Phenyl groups in triphenylphosphine have normal bond properties.

In both the complexes, the C–C and C–N bond distances associated with piperidine in the dithiocarbamate fragment are normal and the piperidine ring is in the chair conformation. The methyl group in the terminal position is equatorially oriented to avoid 1,3-diaxial steric interactions with the axial hydrogens.

Table 1 shows that the S–Ni–S angles are very similar for **1** and **2**. The Ni–S and C–N (thioureide) bond lengths of **2** are shorter than in **1**. The shortening of the Ni–S and C–N bond lengths is a clear manifestation of mesomeric shift of electron density toward nickel through the thioureide C–N bond in **2** compared with **1** because of the presence of π-acidic triphenylphosphine in **2**. As a result of the reduced Ni–S bond length in **2**, the C–S bond length increases and S–C–S angle decreases compared with **1**. The N–C–S and Ni–S–C bond angles are also affected by the π back-bonding effect of the triphenylphosphine in **2**.

Cyclic voltammetric studies

The reduction potential for the parent [Ni(4-mpipdtc)$_2$] (**1**) is observed at −1414 mV. The mixed ligand complex **2** had a lower one-electron reduction potential (−993 mV). The lower reduction potential observed for complex **2** indicates the ease of electron addition in the mixed ligand complex because of the presence of PPh_3 around the nickel atom [22].

Table 1 Comparison of bond distances (Å) and angles (°)

	1	**2**
Ni–S	2.1947(11)	2.187(2)
C–N	1.310(5)	1.282(10)
C–S	1.710(4)	1.723(8)
S–Ni–S	79.10(4)	79.08(8)
S–C–S	109.6(2)	107.8(4)
N–C–S	125.2(3)	126.1(6)
Ni–S–C	85.42(13)	86.6(3)

Based on IR, ^{13}C NMR spectral, and single-crystal X-ray studies, C–N (thioureide) in [Ni(4-mpipdtc)(PPh_3)(NCS)] has maximum double bond character and hence this complex is expected to be more difficult to reduce; in reality, however, it is more easily reduced than the parent [Ni(4-mpipdtc)$_2$], probably because of the extensive π back-bonding with the phosphorus atom which drains the excess negative charge on the metal and hence lowers the reduction potential.

Conclusions

The crystalline compounds **1** and **2** were prepared and studied by electronic, IR, and NMR spectroscopy, cyclic voltammetry, and single-crystal X-ray diffraction. The spectral and single-crystal X-ray structural studies on **1** and **2** indicate that the central metal atom is in a planar environment for both complexes, and the effect of PPh_3 on the

Table 2 Crystal data and refinement values for [Ni(4-mpipdtc)$_2$] (**1**) and [Ni(4-mpipdtc)(PPh_3)(NCS)] (**2**)

	1	**2**
Empirical formula	$C_{14}H_{24}N_2NiS_4$	$C_{26}H_{27}N_2NiPS_3$
Formula weight	407.30	553.36
Temperature (K)	293 (2)	293 (2)
Wavelength (Å)	0.71073	0.71073
Crystal system, space group	Monoclinic, *P*21/C	Triclinic, *P*-1
Unit cell dimensions	$a = 8.6428$ (8) Å	$a = 7.8638$ (4) Å
	$\alpha = 90.000°$	$\alpha = 91.844$ (3)°
	$b = 18.4442$ (17) Å	$b = 16.6609$ (9) Å
	$\beta = 106.609$ (5)°	$\beta = 90.474$ (3)°
	$c = 12.0873$ (10) Å	$c = 20.9558$ (10) Å
	$\gamma = 90.000°$	$\gamma = 92.958$ (3)°
Volume (Å^3)	1846.4 (3)	2740.4 (2)
Z, calculated density (mg m^{-3})	4, 1.465	4, 1.341
Absorption coefficient (mm^{-1})	1.498	1.012
F(000)	856	1152
Crystal size (mm)	0.30 × 0.22 × 0.20	0.30 × 0.20 × 0.20
Theta range for data collection (°)	2.08–25.62	0.97–25.00
Limiting indices	$-10 \le h \le 10$	$-9 \le h \le 9$
	$-22 \le k \le 22$	$-19 \le k \le 19$
	$-14 \le l \le 14$	$-24 \le l \le 24$
Reflections collected	3467	9632
Observed reflections	2477	7326
Absorption correction	Semi-empirical from equivalents	Semi-empirical from equivalents
Maximum and minimum transmission	0.6622 and 0.7538	0.7932 and 0.7112
Refinement method	Full-matrix least squares on F^2	Full-matrix least squares on F^2
Goodness of fit on F^2	1.072	1.280
Final *R* indices ($I > 2$ sigma (I))	$R1 = 0.0704$, $wR2 = 0.1248$	$R1 = 0.0749$, $wR2 = 0.2022$
R indices (all data)	$R1 = 0.0404$, $wR2 = 0.1016$	$R1 = 0.0999$, $wR2 = 0.2233$

mesomeric drift of electron density towards nickel through the thioureide C–N bond. A significant asymmetry in the Ni–S bond in **2** (2.162(2) and 2.211(2) Å) supports the less effective trans effect of SCN^- over PPh_3. CV studies showed a higher reduction potential for the parent complex **1** indicating reluctance to add more electron density to the already electron-rich metal centre.

Experimental

All reagents and solvents were commercially available high-grade materials (Sigma–Aldrich, Sd fine, Spectrochem) and used as received. IR spectra were recorded on a Thermo Nicolet Avatar 330 FT-IR spectrophotometer (range: 400–4,000 cm^{-1}) as KBr pellets. The NMR spectra were recorded on a Bruker 500 MHz NMR spectrometer at room temperature in $CDCl_3$ using TMS as internal reference. A CH Instruments chi604c electrochemical analyzer was used to record the cyclic voltammograms of the complexes. The working electrode was made of platinum. The counter electrode was a platinum wire and the reference electrode was Ag/AgCl. Pure dichloromethane was used as the solvent. The supporting electrolyte was tetrabutylammonium perchlorate. The experimental solution was thermostated at 28 ± 1 °C in an oxygen-free atmosphere provided by bubbling nitrogen through the solution.

X-Ray crystallography

Details of the crystal data and structure refinement values for complexes **1** and **2** are summarized in Table 2. The intensity data were collected at ambient temperature on a Bruker axis Kappa apex 2 CCD diffractometer using graphite monochromated Mo-K_α radiation ($\lambda = 0.71073$ Å). The

Table 3 Selected bond lengths (Å) and angles (°) for complexes **1** and **2**

1		**2**			
		Molecule A		Molecule B	
C1-N1	1.308(5)	C19-S2	1.721(8)	C45-S5	1.714(8)
C1-S2	1.711(4)	C19-S1	1.725(7)	C45-S4	1.730(7)
C1-S1	1.712(4)	C26-S3	1.616(9)	C52-S6	1.611(8)
C2-N2	1.311(4)	P1-Ni1	2.1878(19)	P2-Ni2	2.1904(19)
C2-S3	1.707(4)	S1-Ni1	2.162(2)	S4-Ni2	2.162(2)
C2-S4	1.709(4)	S2-Ni1	2.211(2)	S5-Ni2	2.215(2)
C3-N1	1.457(5)	N2-Ni1	1.868(7)	N4-Ni2	1.862(7)
C7-N1	1.464(5)	C6-C1-P1	118.6(5)	C32-C27-P2	122.5(6)
S1-Ni1	2.1964(10)	C2-C1-P1	122.7(6)	C28-C27-P2	120.0(6)
S2-Ni1	2.1923(11)	N1-C19-S2	125.7(6)	N3-C45-S5	126.6(6)
S3-Ni1	2.2009(11)	N1-C19-S1	126.5(6)	N3-C45-S4	125.5(6)
S4-Ni1	2.1892(11)	S2-C19-S1	107.8(4)	S5-C45-S4	107.9(4)
N1-C1-S2	125.1(3)	N2-C26-S3	108.6(7)	N4-C52-S6	177.9(8)
N1-C1-S1	125.3(3)	C26-N2-Ni1	173.3(7)	C52-N4-Ni2	171.1(7)
S2-C1-S1	109.5(2)	C7-P1-C13	106.8(3)	C33-P2-C27	106.8(3)
N2-C2-S3	125.9(3)	C7-P1-C1	103.5(3)	C33-P2-C39	105.0(3)
N2-C2-S4	124.4(3)	C13-P1-C1	104.9(3)	C27-P2-C39	103.8(3)
S3-C2-S4	109.7(2)	C7-P1-Ni1	107.8(2)	C33-P2-Ni2	113.9(2)
C1-S1-Ni1	85.37(12)	C13-P1-Ni1	114.0(2)	C27-P2-Ni2	108.0(2)
C1-S2-Ni1	85.51(13)	C1-P1-Ni1	118.8(2)	C39-P2-Ni2	118.5(2)
C2-S3-Ni1	85.23(13)	C19-S1-Ni1	87.3(3)	C45-S4-Ni2	87.2(3)
C2-S4-Ni1	85.55(12)	C19-S2-Ni1	85.8(3)	C45-S5-Ni2	85.9(3)
S4-Ni1-S2	100.07(4)	N2-Ni1-S1	171.7(2)	N4-Ni2-S4	171.4(2)
S4-Ni1-S1	177.22(5)	N2-Ni1-P1	91.10(19)	N4-Ni2-P2	91.5(2)
S2-Ni1-S1	79.16(4)	S1-Ni1-P1	96.22(8)	S4-Ni2-P2	96.18(7)
S4-Ni1-S3	79.04(4)	N2-Ni1-S2	94.34(19)	N4-Ni2-S5	94.07(19)
S2-Ni1-S3	173.89(4)	S1-Ni1-S2	79.08(8)	S4-Ni2-S5	78.99(8)
S1-Ni1-S3	101.44(4)	P1-Ni1-S2	169.11(11)	P2-Ni2-S5	169.39(9)

structures were solved by SIR 92 [23] and refined by full matrix least-squares with SHELXL-97 [24]. All non-hydrogen atoms were refined anisotropically and the hydrogens were fixed geometrically. Selected bond distances and angles are listed in Table 3. Crystallographic data have been deposited with the Cambridge Crystallographic Data Centre as supplementary publications numbers CCDC-720377 and 693200 for **1** and **2**, respectively. Copies of the data can be obtained free of charge on application to CCDC, 12 Union Road, Cambridge CBZ 1EZ, UK.

*Preparation of [Ni(4-mpipdtc)$_2$] (**1**)*

An aqueous solution of 2.37 g $NiCl_2{\cdot}6H_2O$ (10 mmol) was added to an aqueous solution of 3.92 g sodium 4-methylpiperidinedithiocarbamate (20 mmol) with constant stirring. The solid which precipitated was washed several times with cold water and dried. Results from analysis of the complex were in agreement with [Ni(4-mpipdtc)$_2$] [25]. IR (KBr): $\bar{\nu}$ = 1,510 (C–N), 946 (C–S) cm^{-1}; ^{1}H NMR (500 MHz, $CDCl_3$): δ = 0.98 (CH_3, d), 1.18–1.25 (H-4, m), 1.70–1.77 (H-3, m), 2.93 (H-2 axial, t), 4.51 (H-2 equatorial, d) ppm; ^{13}C NMR (125 MHz, $CDCl_3$): δ = 21.28 (CH_3), 29.68 (C-3), 33.37, 30.86 (C-4), 46.84 (C-2), 204.85 (NCS_2) ppm.

*Preparation of [Ni(4-mpipdtc)(PPh$_3$)(NCS)] (**2**)*

A mixture of 0.202 g Ni(4-mpipdtc)$_2$ (0.5 mmol), 0.260 g PPh_3 (1 mmol), 0.120 g $NiCl_2{\cdot}6H_2O$ (0.5 mmol), and 0.076 g NH_4SCN (1 mmol) was heated under reflux for 3 h in 50 cm^3 CH_2Cl_2–CH_3CN (1:1). The purple red solution obtained was filtered and left for evaporation. After 4 days, fine crystals suitable for X-ray structural analysis were obtained. Results from analysis of the complex were in agreement with [Ni(4-mpipdtc)(PPh_3)(NCS)]. IR (KBr): $\bar{\nu}$ = 1,544 (C–N), 965 (C–S), 2,098 (C≡N), 848 (C–S(NCS)) cm^{-1}; ^{1}H NMR (500 MHz, $CDCl_3$): δ = 0.98 (CH_3, d), 1.01–1.25 (H-4, m), 1.57–1.82 (H-3, m), 2.92 (H-2 axial, t), 4.50

(H-2 equatorial, d), 7.43–7.74 (PPh_3) ppm; ^{13}C NMR (125 MHz, $CDCl_3$): $\delta = 21.20$ (CH_3), 30.60 (C-3), 33.34 (C-4), 46.98 (C-2), 128.47–132.30 (PPh_3), 201.06 (NCS_2) ppm.

Acknowledgments We are thankful to SAIF, Indian Institute of Technology, Madras for the single crystal X-ray structural analysis.

References

1. Cox MJ, Tiekink ERT (1997) Rev Inorg Chem 17:1
2. Heard J (2005) Prog Inorg Chem 53:1
3. Nan Y, Yang Z (1999) Tetrahedron Lett 40:2323
4. Srogl J, Liu W, Marshall D, Liebeskind LS (1999) J Am Chem Soc 121:9449
5. Sambaiah T, Li L, Huang D, Lin C, Rayabarapu DK, Cheng C (1999) J Org Chem 64:3663
6. Jarrett PS, Dhubhghaill OMN, Sadler PJ (1993) J Chem Soc Dalton Trans 1863
7. Bonamico M, Destry G, Mariani C, Vaciago A, Zambonelli L (1965) Acta Crystallogr B 19:619
8. Uppadine LH, Weeks JM, Beer PD (2001) J Chem Soc Dalton Trans 3367
9. Chakrawarty A (1966) Prog Inorg Chem 7:83
10. Fackler JP Jr, Seigel WC (1969) Inorg Chem 8:1631
11. Jorgensen CK (1964) Inorg Chem 3:1201
12. Ramalingam K, Aravamudan G, Venkatachalam V (1993) Bull Chem Soc Japan 66:1554
13. Arul Prakasam B, Ramalingam K, Saravanan M, Bocelli G, Contoni A (2004) Polyhedron 23:77
14. Bonati F, Ugo R (1967) J Organomet Chem 110:257
15. Cernickova JE, Chartonik IA, Umrejko DS, Kavirikov VI (1989) Coord Chem 15:1695
16. Lever ABP (1968) Inorganic electronic spectroscopy. Elsevier, Amsterdam, p 343
17. Tsipis CA, Meleziadis IJ, Kessissoglou DP, Kotsolos GA (1984) Inorg Chim Acta 90:L19
18. Arulprakasam B, Ramalingam K, Bocelli G, Cantoni A (2007) Polyhedron 26:4489
19. Ivanov AV, Roduia T, Antzutkin ON (1998) Polyhedron 17:3101
20. Higgins GMC, Saville B (1963) J Chem Soc 2812
21. Ramalingam K, Radha K, Aravamudan G, Mahadevan C, Subramaniyam CH, Seshasayee M (1984) Acta Crystallogr C 40:1838
22. Ramalingam K, Aravamudan G, Seshasayee M (1987) Inorg Chim Acta 128:231
23. Ahomre A, Burla ML, Camalli M, Cascavano G, Giacovazzo G, Gugaliardi A, Polidori G (1994) J Appl Crystallogr 27:4385
24. Sheldrick GM (1997) SHELXL 97. University of Göttingen, Göttingen
25. Fabretti AC, Franchini GC, Pretic C, Toshi G, Zannini P (1985) Transit Met Chem 10:284